Edwin M. Perkins* and Karen D. Rosenthal

HISTOPATHOLOGY OF CADMIUM-EXPOSED SCORPIONFISH

The histopathological investigations described here were primarily intended to test the hypothesis that no tissue damage will result if cadmium is completely detoxified. About 280 slides were examined of 1) gill, intestine, liver, and kidney tissue of scorpionfish exposed for 4-, 8-, and 16-week periods to 0.1 and 1.0 ppm of ionic cadmium and 2) controls. Although various lesions were found, they appear to have arisen from unknown causes and none can be correlated with the exposures to cadmium. Moreover, some of the lesions that previously were ascribed to 50-ppm cadmium exposures by Gardner and Yevich (1970) were found in the nonexposed animals.

MATERIALS AND METHODS

Necropsies were performed on 70 adult California scorpionfish *(Scorpaena guttata Girard)* collected off Anacapa Island. All ranged between 18.4 and 32.1 cm in standard length.

Gill, intestine, kidney, and liver samples were excised and fixed in 10% neutral buffered formalin. Tissues were then dehydrated, infiltrated, and embedded in paraffin. Sections were cut at 6 μ on a rotary microtome and then stained with Harris' hematoxylin and eosin (Humason 1972). Selected samples of liver were also treated according to the periodic acid-Schiff method for the demonstration of glycogen (Luna 1968). Other liver samples were fixed in gluteraldehyde, postfixed in osmium tetroxide, embedded in resin, sectioned, and examined by transmission electron microscopy.

*Marine Biology Research Section, Department of Biological Sciences, University of Southern California, Los Angeles.

All slides were then appraised by light microscopy, using a "blind" rating system that assigned code numbers to each respective specimen; in this way, exposures and times were not revealed to the authors until after the pathological reports had been completed. Criteria and terminology employed for histopathological interpretation were based largely on the works of Ribelin and Migaki (1975), Roberts (1978), Malins et al. (1980), McCain et al. (1982), and Yasutake and Wales (1983). Initially, evaluations of gills, intestines, kidneys, and livers were based on observations made from seven control fish. Thereafter, comparable histological and/or histopathological data were recorded from nine other subsets of seven fish each: i.e., 4-, 8- and 16-week controls, 4-, 8- and 16-week 0.1-ppm cadmium exposures, and 4-, 8- and 16-week 1.0-ppm cadmium exposures. Numerical results from these histological evaluations were analyzed statistically by means of the Kruskal-Wallis Test. This test is a nonparametric statistical method that extends Wilcoxon's Rank Sum Test to greater than two populations of data and provides a chi-square approximation (Lyman 1977). The data analyses were performed using Statistical Analysis Systems (SAS) software (Cary 1982).

RESULTS AND DISCUSSION

This section describes the frequency of occurrence of normal and pathological conditions in control and cadmium-exposed scorpionfish. A pictorial glossary follows in which the details of the observed conditions are described. As will be shown below, no pathological conditions could be related to cadmium exposure. This may be because most cadmium was successfully detoxified by metallothionein in exposed scorpionfish and, as a result, the amount of spillover of cadmium into the enzyme-containing (ENZ) pool was insufficient to result in tissue-level pathology (Bay et al., this volume(a); Brown et al., this volume).

Gill

Figure 1 summarizes the incidence of major gill lesions recorded during this study. Although lamellar hypertrophy (Figure 1a) tended to increase slightly over time, lamellar hyperplasia (Figure 1b) did not. Lamellar fusion (Figure 1c), by contrast, appeared only in those fish placed in holding tanks; i.e., it was not observed in any of the initial, 0-week control organisms. Furthermore, when lamellar fusion did become apparent among 4-, 8- and 16-week groupings, no clearcut or decipherable patterns emerged; e.g., the incidence of lamellar fusion peaked among those control organisms not exposed to cadmium during week 8, whereas it remained relatively constant among the 4-, 8- and 16-week 0.1-ppm cadmium-exposed groups and actually declined somewhat in the 1.0-ppm cadmium-exposed fish. Whatever the explanation, cadmium can be ruled out as the contributory factor.

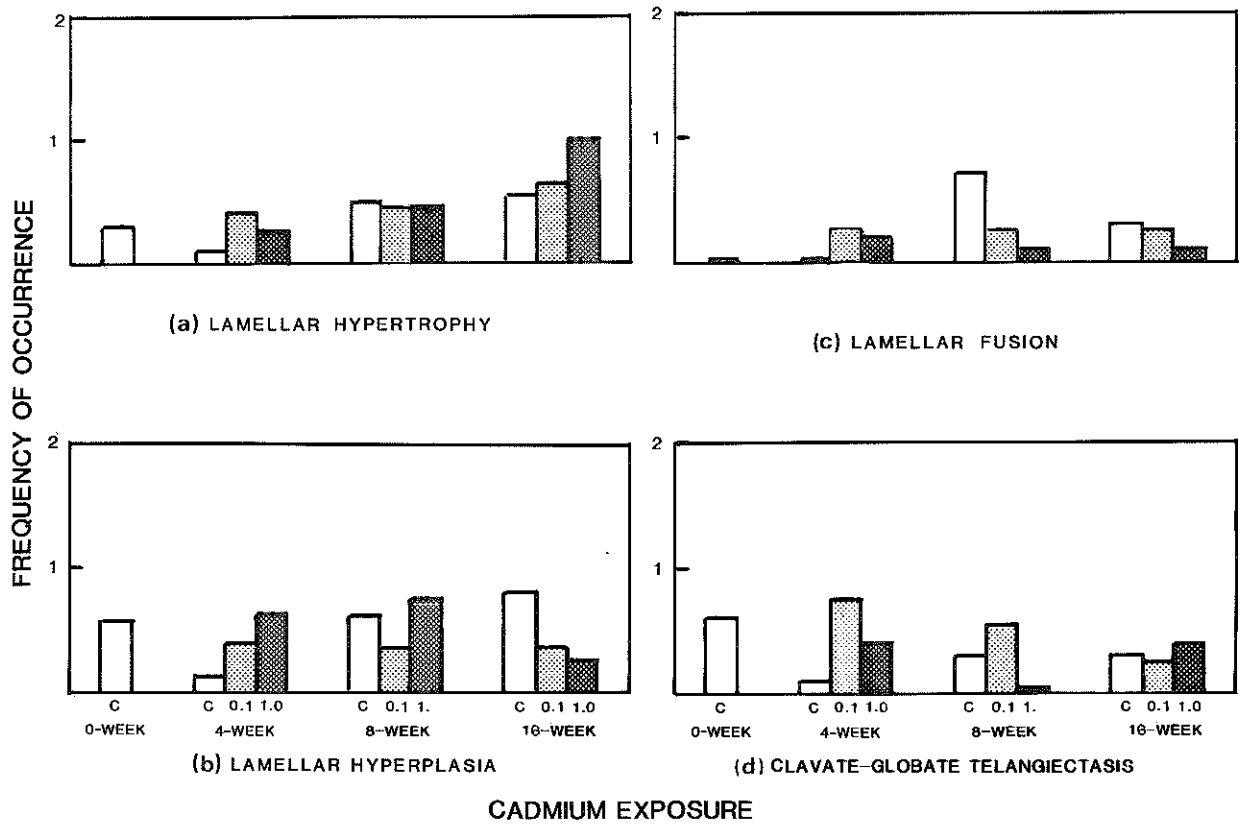

Figure 1. Incidence of representative idiopathic lesions in scorpionfish gill.

Intestine

Intestinal idiopathies (Figure 2) failed to exhibit any statistically significant trend other than intracytoplasmic epithelial vacuolation (Figure 2d). Note that the incidence of this lesion among initial, 0-week controls overshadows that observed in all 4-, 8- and 16-week groupings. This would suggest that if this condition existed in the natural environment of these organisms prior to capture, then so too did its cause.

Kidney

Major renal lesions are depicted graphically in Figure 3. In that respective enzyme-cadmium levels were probably too low to account for any metabolic effects (Bay et al., this volume(b)), all idiopathies likely evolved as a consequence of some other, as yet unknown, factor or factors. Vacuolar degeneration of the proximal tubule (Figure 3a) could be indicative of osmoregulatory difficulties experienced by the fish, given that comparable lesions have earlier been reported as "osmotic nephrosis."

A more gradual, temporal trend towards abnormalcy is represented by

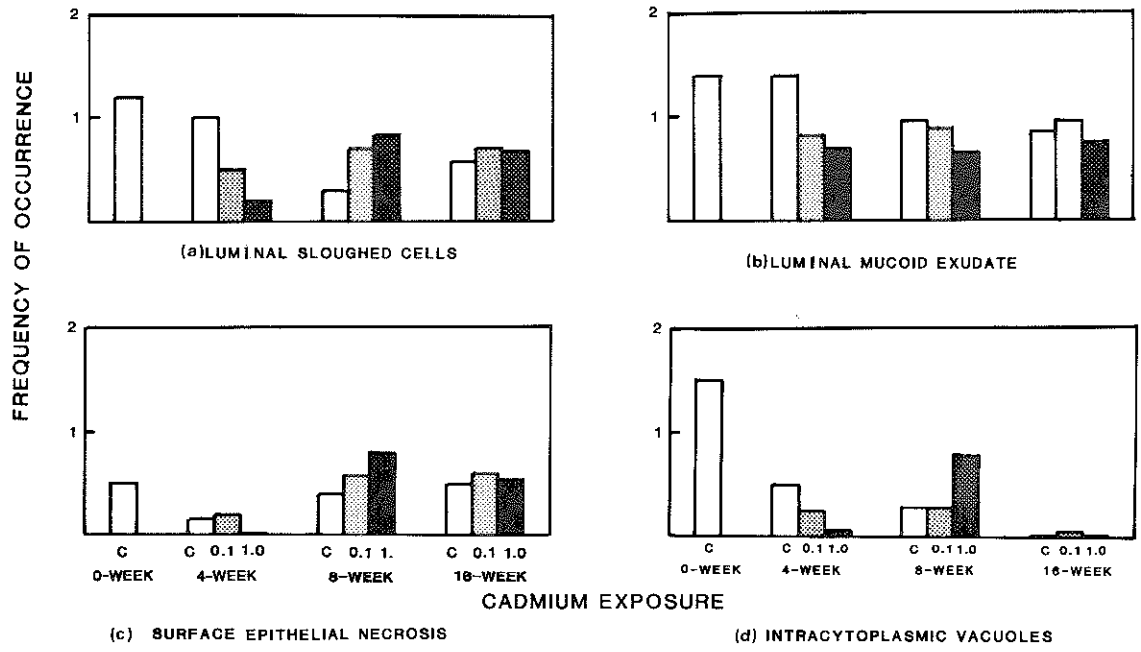

Figure 2. Occurrence of selected idiopathies in scorpionfish intestine.

the increased thickening of parietal epithelium in Bowman's capsule (Figure 3b). This tendency is particularly pronounced among the 4-, 8- and 16-week 1.0-ppm cadmium-exposed organisms. By contrast, the onsets of both megalocytosis/megalokaryosis (Figure 3c) and periarteriolar fibrinoid degeneration (Figure 3d) did not occur until week 8--the former being precipitous, the latter, gradual.

Also of statistical significance in the kidney was the inverse relationship between numbers and sizes of melanin macrophage centers (Figure 4). Whereas quantities peaked among each subset of seven experimental organisms during week 8, dimensions were reduced. Although this correlation had earlier been reported in the livers of plaice exposed to crude oil (Haensly et al. 1982), our study confirmed it only in the kidney (Figure 5).

Liver

Representative changes detected in scorpionfish livers are illustrated in Figure 6. The incidence of hepatocyte hypertrophy (Figure 6a) increased with statistical significance within and among all groups throughout this experiment. The fatty vacuolation of hepatocytes, however, remained moderately high from the onset (Figure 6b). Inexplicably, the degree of venous sinusoidal congestion paralleled neither hepatocyte hypertrophy nor vacuolation during week 16 (Figure 6c). As noted earlier in the kidney, certain hepatic idiopathies did not occur until weeks 8 and 16: these included hepatocellular nuclear

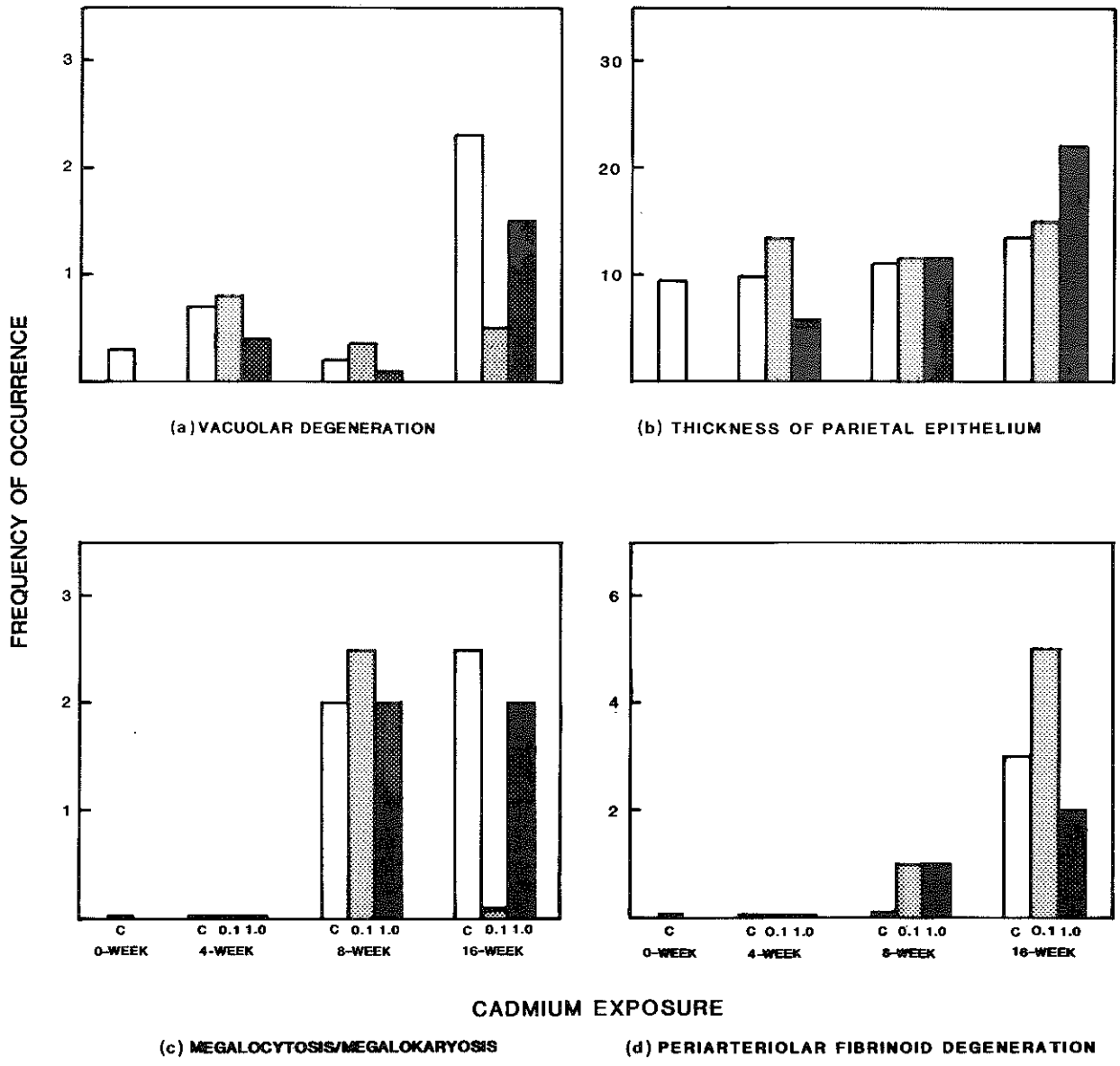

Figure 3. Prevalence of representative idiopathic lesions in scorpionfish kidney.

pleomorphism, nuclear pyknosis, sclerotic foci, focal hepatocellular necrosis (degenerative foci), and hyperplastic foci (Figure 6d).

CONCLUSIONS

Various idiopathic lesions have been documented during this experiment, yet none can be correlated with those subacute levels of cadmium to which the scorpionfish were exposed. That some of these lesions occurred with equal or higher frequency among initial, 0-week control organisms (necropsied at the beginning of the experiment, after a 4-week acclimation period) only serves to emphasize the need for caution

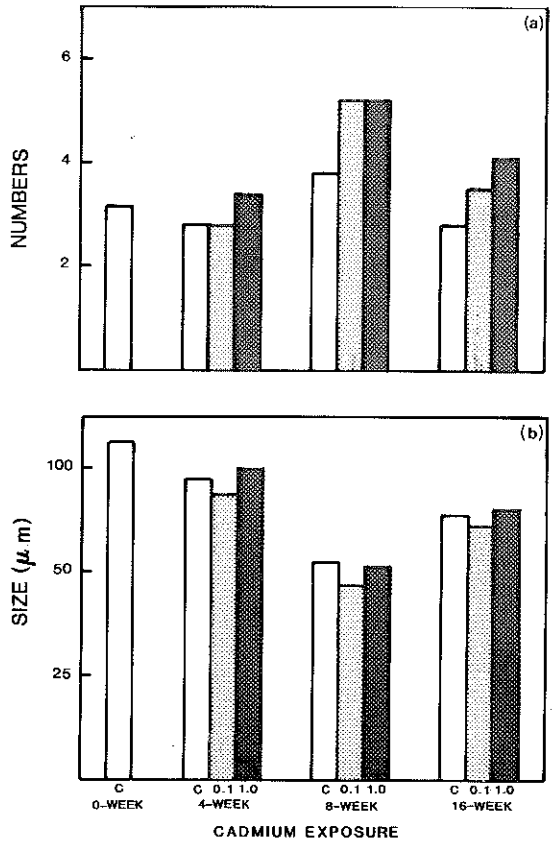

Figure 4. Numbers (a) and sizes (b) of renal melanin macrophage centers.

when attempting to establish cause-and-effect relationships between etiological contaminants and observed pathologies. It also stresses the need to use animals in the laboratory that have not been previously exposed to other contaminants. Indeed, some of the initial, 0-week control fish used in this study exhibited everything from gill lamellar hypertrophy, hyperplasia, lymphocytic infiltration, and clavate-globate telangiectasis to intestinal epithelial necrosis, sloughing, intracytoplasmic vacuolation, edema, and copious mucoid exudate. Others possessed renal tubular degeneration, thickened parietal epithelium, membranous glomerulonephritis, hepatocyte hypertrophy, vacuolation, and sinusoidal congestion. It is discomforting to note that many of those lesions which are classically ascribed to 50-ppm cadmium exposures fall also into the preceding nonexposure categories (cf: Gardner and Yevich 1970).

For this reason, a number of other factors must also be taken into account. Consider, for example, the difficulty of appraising natural morphological and physiological variations within members of a given species--not to mention between members of different but closely allied species. Adequate sample sizes and accurate taxonomic determinations

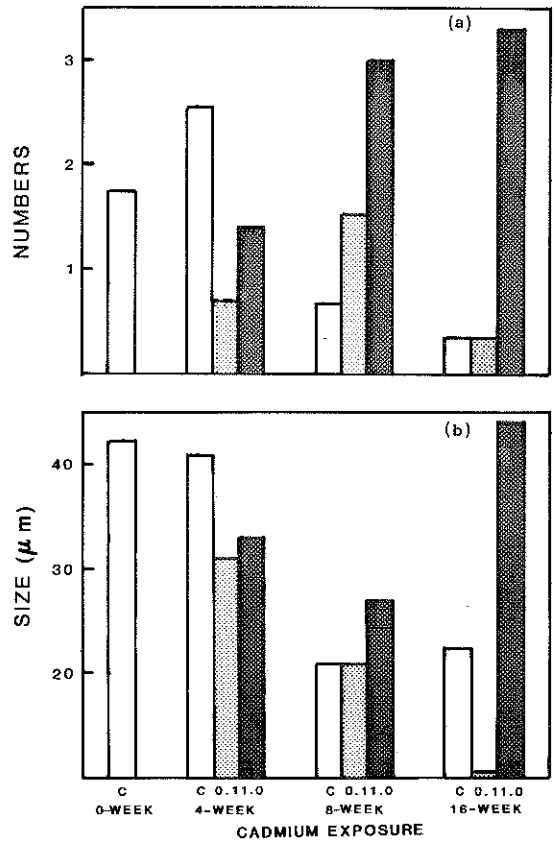

Figure 5. Numbers (a) and sizes (b) of hepatic melanin macrophage centers.

are therefore of utmost importance. So, too, is the standardization of laboratory methodologies: different fixatives, different hematoxylin and eosin regimens, and different tissue section thicknesses produce very different microscopic images. And even if these images were interpreted in like manner by different individuals, it is doubtful that there would be any consensus of opinion because current criteria and nonmenclature regarding nonmammalian histopathology also lack standardization.

Seasonality is another factor that must always be considered. For example, we do not know how to interpret the unusually high occurrence of either intestinal epithelial intracytoplasmic vacuolation (Figure 2d) or hepatocellular lipid vacuolation (Figure 6b), both of which prevailed in this experiment's control organisms. They may be normal reflections of dietary patterns (cf: Slooff et al. 1983) and/or reproductive cycles, or they may be pathological manifestations of metal and/or chlorinated hydrocarbon contamination. This issue cannot be resolved on the basis of chemical analyses alone; monthly sampling of specimens over a 1-year period must also be employed if seasonality is to be precluded.

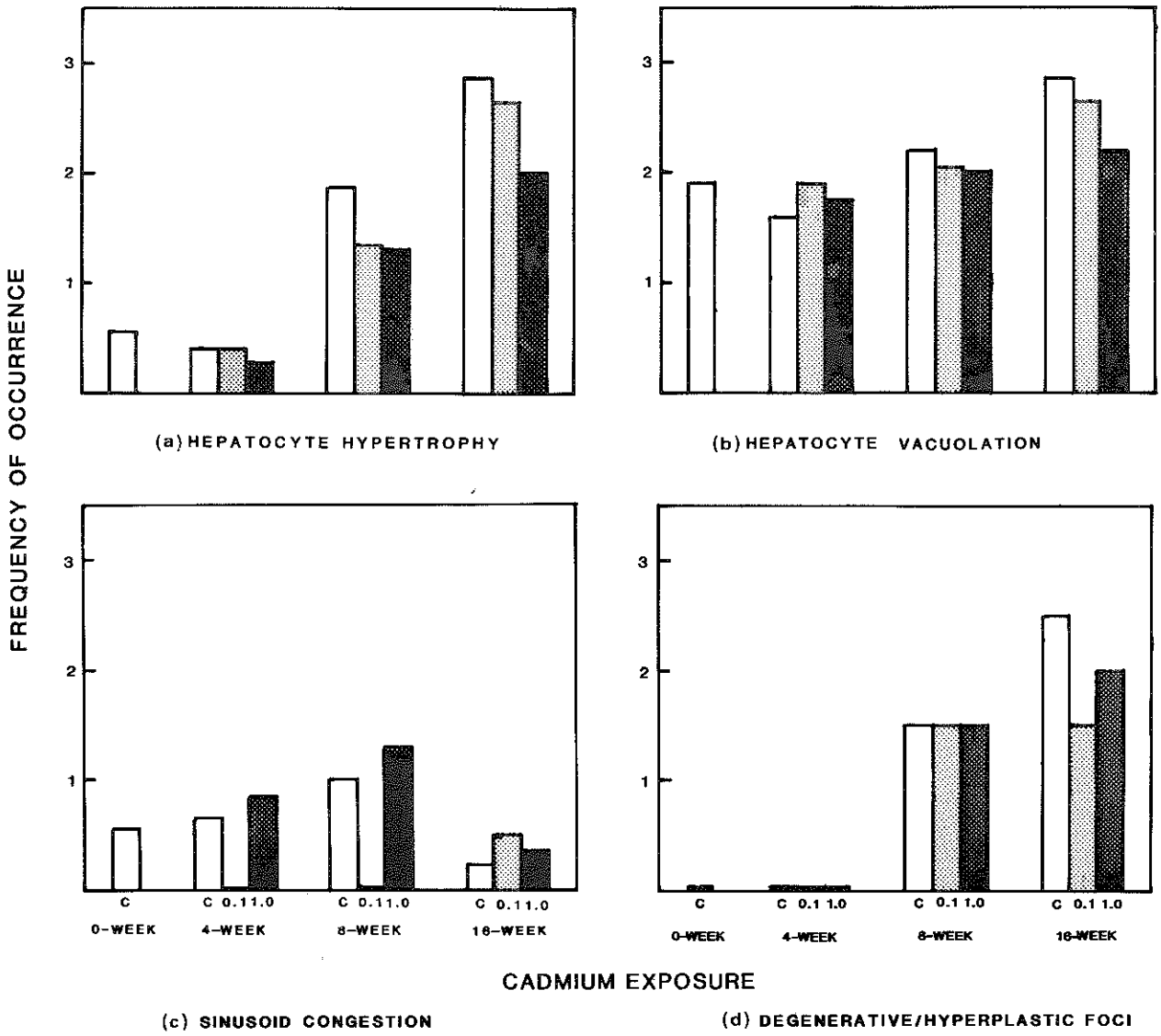

Figure 6. Frequencies of selected idopathies in scorpionfish liver.

One final insight into the origin of idiopathies concerns their time of onset. Some, as exemplified by hepatocellular lipid vacuolation, were acquired in situ; others, however, developed subsequent to collection--in other words, they arose either as a direct result of the sampling method or as an indirect result of stress induced by holding tanks. Intraluminal hemorrhagic exudate in the renal collecting tubules--also known as "shock kidney," lamellar gill fusion (Figure 1c), periarteriolar fibrinoid degeneration (Figure 3d), and hepatocellular degenerative foci (Figure 6d) can all be relegated to this latter category (see also Figures G9, G3, and G17, respectively, in the glossary below). Therefore, in order to better sort out the origins of such lesions, it is essential to monitor holding tank variables including water temperature, water chemistry, space requirements, and artificial diet.

In summary, the results presented in this report clearly demonstrate the need to account for additional parameters in all future studies--seasonal cycles, effects of captivity, and variations between individuals--if histopathologists are to interpret idiopathic lesions accurately and expeditiously.

PICTORIAL GLOSSARY OF NORMAL TISSUES AND IDIOPATHIC LESIONS

Lesions found within the gill, intestine, kidney, and liver tissue of the cadmium-exposed and control scorpionfish examined in this study are described and illustrated below. Descriptions of normal tissues are included for comparison.

Gill

Normal, unaffected gills are composed of cartilaginous primary lamellae; extending from these are multiple numbers of epithelium-covered secondary lamellae (Figure G1). Traversing the length of each secondary lamella is a tiny blood capillary, derived from the branchial artery. Numbers of mucus-producing cells may be observed throughout; however, their occurrence is greatest at the base of each gill stem. The most prevalent tissue alterations observed during this study were hyperplasia and hypertrophy, lamellar fusion, clavate-globate telangiectasis, and parasitism.

Hyperplasia and Hypertrophy. This condition is characterized by a marked increase in numbers of constituent cells (hyperplasia), which accounts for an overall increase in size (hypertrophy) of the involved lamellae (Figure G2).

Lamellar Fusion. Presumably caused by chronic inflammatory response, lamellar fusion is typified by contiguous secondary lamellae that are devoid of free surfaces except at their apices (Figure G3). Although the blood capillaries of these secondary lamellae persist individually, their thickened and metaplastic surface epithelium is continuous.

Clavate-Globate Telangiectasis. This idiopathy involves the distal components of secondary lamellar capillaries, which are greatly dilated (telangiectasis) and therefore distorted into leaflike or clublike (clavate-globate) shapes (Figure G4). Equivalent to capillary aneurysms, they topographically occur in random fashion.

Parasitism. Monogentic trematodes were the most common gill parasite observed. Usually represented by immature stages of their life cycle, occasional adults could also be seen affixed to their host's secondary lamellae (Figure G5).

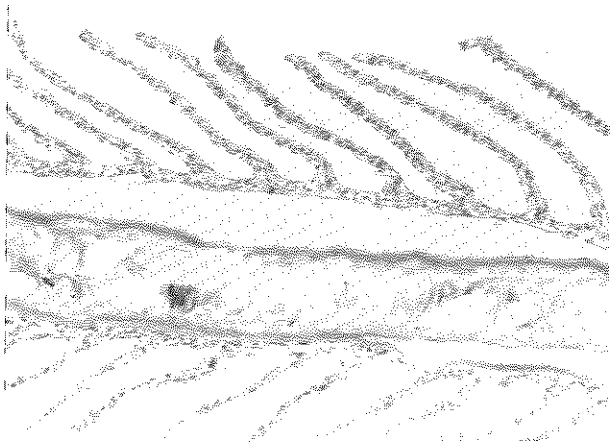

Figure G1. Normal gill: 4W:0.1 (4-week, 0.1-ppm cadmium-exposed fish) x100.

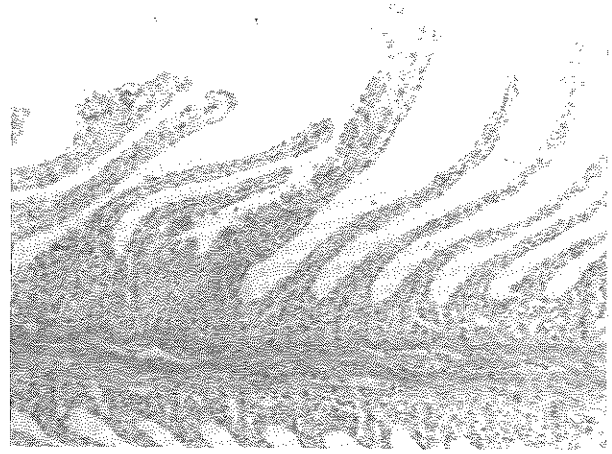

Figure G2. Lamellar hyperplasia and hypertrophy: 4W:1.0 x100.

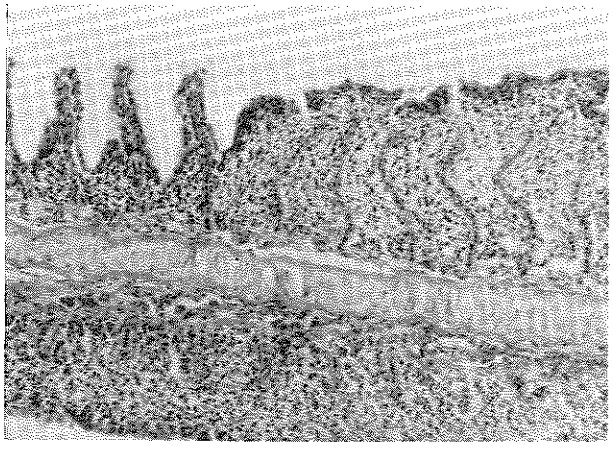

Figure G3. Lamellar fusion: 4W:1.0 x100.

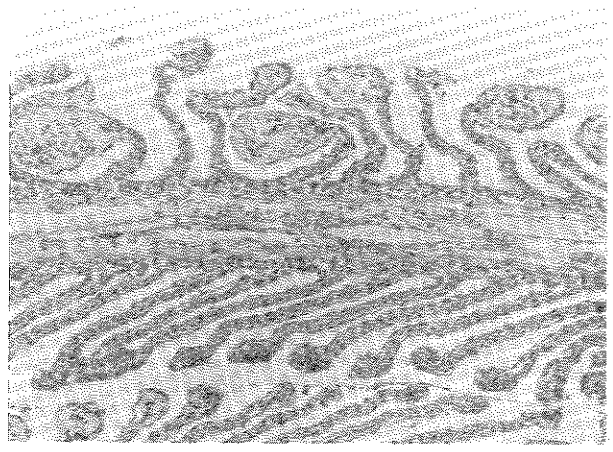

Figure G4. Clavate-globate telangiectasis: 4W:0.1 x100.

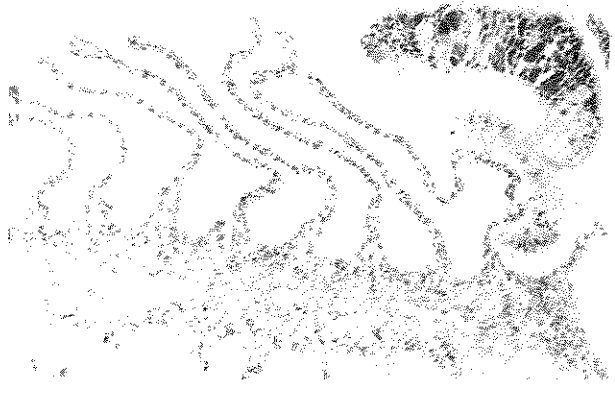

Figure G5. Monogenetic trematode, affixed to secondary gill lamella: 8W:0.1 x100.

Intestine

In cross section, the appearance of normal scorpionfish intestine assumes an innermost series of mucosal infoldings that surround a central lumen (Figure G6). Each infolding or fingerlike projection is covered with simple columnar epithelium. Although some of this epithelium consists of mucus-producing goblet cells and the enigmatic rodlet cells, most is composed of cells that subserve an absorptive function--as is denoted by their microvillar brush border. Beneath the epithelium's basal lamina is a lamina propria, rich in areolar connective tissue, blood capillaries, and distal lymphatic lacteals. A more peripheral and well-defined muscularis externa (consisting of inner circular and outer longitudinal smooth muscle) is also present, as is a definite serosa.

Few abnormal conditions were observed in intestines during the course of this experiment. Among these, only necrotic epithelial sloughing and excessive luminal mucoid exudate will be described. Other conditions included marked epithelial vacuolation, inflammatory response in the lamina propria, the exaggerated dilation of lacteals, and intraepithelial parasite infestation by myxosporidian sporozoan protozoans.

Necrotic Epithelial Sloughing. Whereas the rapid mitotic turnover rate of intestinal epithelium is usual, the wholesale sloughing of epithelium--with subsequent denudation of the mucosa--is not (Figure G7). This condition was usually accompanied by the loss of lamina propria.

Excess Luminal Mucoid Exudate. Copious amounts of a mucoid substance were sometimes noted in the intestinal lumen (Figure G7). The quantity of such mucus, which was often admixed with cellular debris, closely paralleled the degree of necrotic epithelial sloughing.

Kidney

The nephron and collecting ducts of a scorpionfish kidney reside in a rich milieu of hemopoietic tissue somewhat analogous to bone marrow. Each nephron consists of a renal corpuscle, composed of Bowman's capsule and the capillary glomerulus that it invests (as in Figure G13. below).*

*Prior to this study, kidneys of all members of the Family Scorpaenidae were thought to be aglomerular (Hickman and Trump 1969).

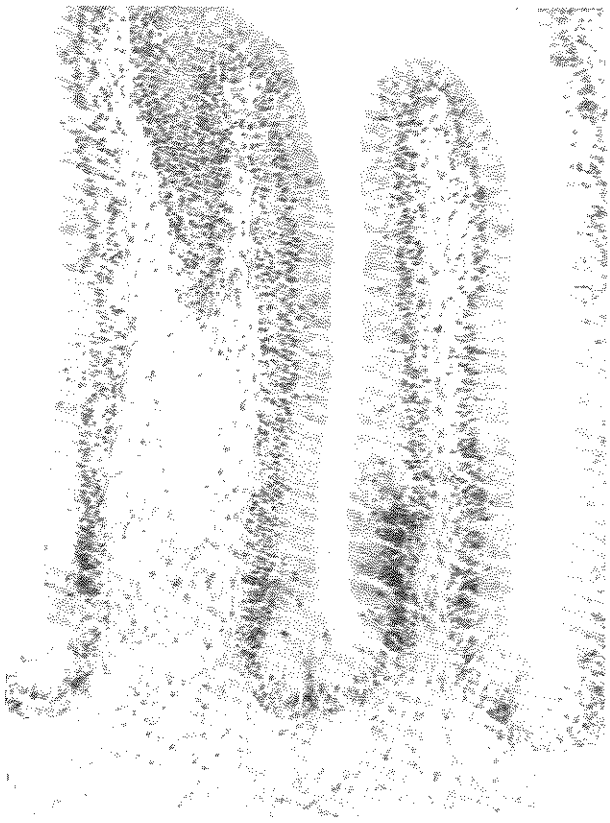

Figure G6. Normal intestine: 16W:0.1 x100.

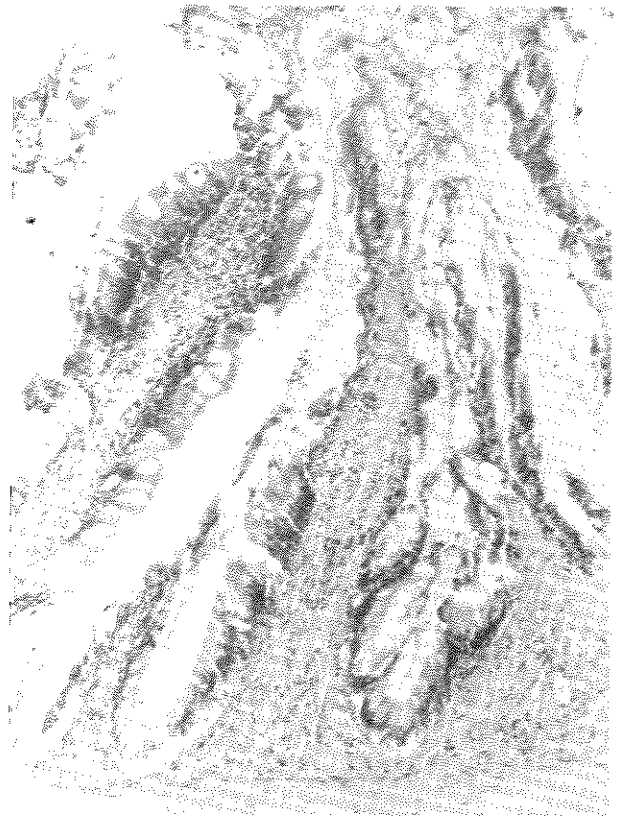

Figure G7. Necrotic, sloughing intestinal epithelium with luminal mucoid exudate: 4W:C (4-week, control fish) x100.

The lumen of Bowman's capsule (called Bowman's space) is, in turn, continuous with the lumen of the remainder of the nephron (i.e., a proximal tubule and perhaps a distal tubule, as in Figure G10 below).* The terminal portion of the nephron then merges with a collecting tubule (Figure G8), which culminates as a mesonephric duct.

Because considerable renal pathology concerns changes in composition of the renal corpuscle, an abbreviated review of normal morphology is given here in order to make clearer the following discriptions of idiopathic lesions. Bowman's capsule consists of an outer, peripheral layer of simple squamous cells (parietal epithelium) and an inner layer of specialized cells (visceral epithelium) that involutes to invest the capillary glomerulus. Additional cells, which contribute to the structural framework of the glomerulus, are collectively termed the

*Although resolution afforded by light microscopy suggests the presence of a proximal tubule (divided into a thin or neck segment, followed by first and second main segments) as well as the existence of a distal tubule, further ultrastructural investigation and confirmation are required.

mesangium or mesangial matrix (Figure G13). That point on a renal corpuscle where the afferent arteriole enters into and/or the efferent arteriole emerges from the endothelial-lined capillary glomerulus is called the vascular pole (Figure G13). At the other end is the urinary pole, a region where the lumen of Bowman's space is continuous with the neck portion of the proximal convoluted tubule (as in Figure G17, below).

Scorpionfish kidneys exhibited the broadest spectrum of pathologic changes. These ranged from luminal hemorrhagic exudates, vacuolar degeneration, and megalokaryosis/megalocytosis, to mesangiolysis, mesangiosclerosis, membranous glomerulonephritis, and periarteriolar fibrinoid degeneration.

Hemorrhagic Exudates. The occurrence of intraluminal hemorrhagic exudates was restricted to collecting tubules and mesonephric ducts (compare Figures G8 and G9). None were observed in components of the nephron. All affected tubules and ducts were markedly distended, and their epithelium was often necrotic.

Vacuolar Degeneration. This lesion is apparently restricted to the first portion of the proximal tubules. In early stages, discrete eosinophilic vacuoles are dispersed throughout the tubular epithelial cytoplasm. As the condition progresses, these vacuoles or droplets appear to coalesce. The terminal stage consists of an enlarged, circumscribed aggregate of clear to eosinophilic vacuoles that are delimited peripherally by the basal lamina of the involved tubule (compare Figures G10 and G11).

Megalokaryosis/Megalocytosis. As is implied by their names, these two conditions manifest themselves as greatly enlarged nuclei and cells, respectively. Either phenomenon is readily apparent when compared to the normal morphology of neighboring cells (Figure G12). Thus far, megalokaryosis and megalocytosis have been observed only in proximal and collecting tubules of scorpionfish kidney.

Mesangiolysis. A degenerative lesion of the renal corpuscle, mesangiolysis is characterized by a swelling or "ballooning" of those components that occupy Bowman's space (Figure G14). Collectively referred to as the glomerular tuft, these include the capillary glomerulus (whose lumina are either dilated or obliterated), the mesangium (which is edematous and/or degenerative), and the visceral epithelium (whose structural integrity is lost).

Mesangiosclerosis. Hallmarks of this renal corpuscular lesion include hypercellularity of the mesangial matrix, fibrous adhesions between visceral and parietal epithelium, and sclerosis peripheral to the parietal epithelium's basal lamina. The latter condition causes the capsule to appear distinctly thickened (Figure G15).

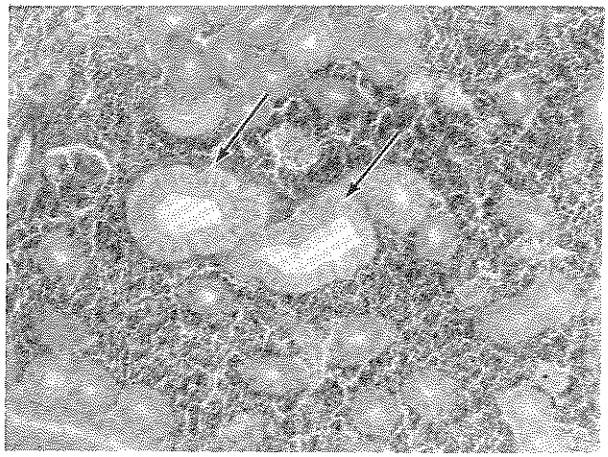

Figure G8. Normal renal collecting tubules (arrows): 4W:1.0 x100.

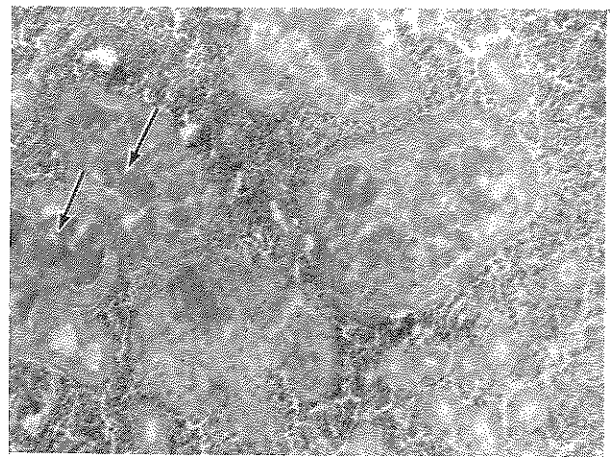

Figure G9. Intraluminal hemorrhagic exudates in renal collecting tubules (arrows): 4W:C x100.

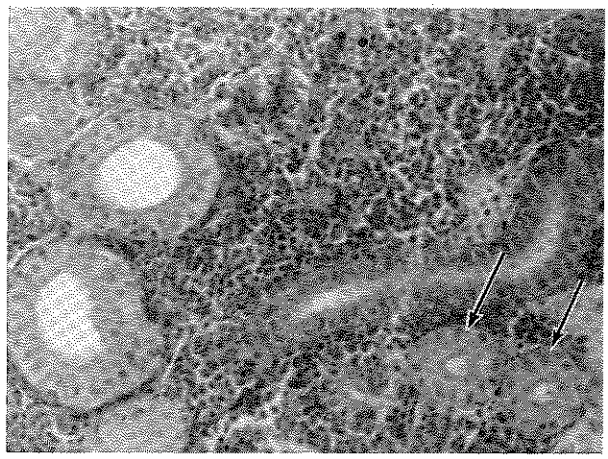

Figure G10. Normal, first-portion proximal tubules in kidney (arrows): 4W:1.0 x200.

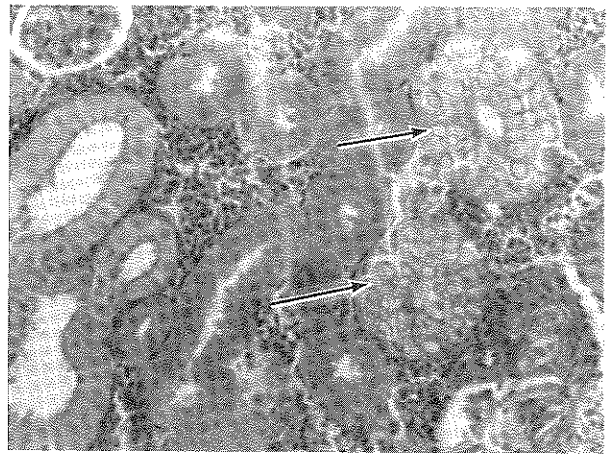

Figure G11. Vacuolar degeneration in first portion of renal proximal tubules (arrows): 4W:0.1 x200.

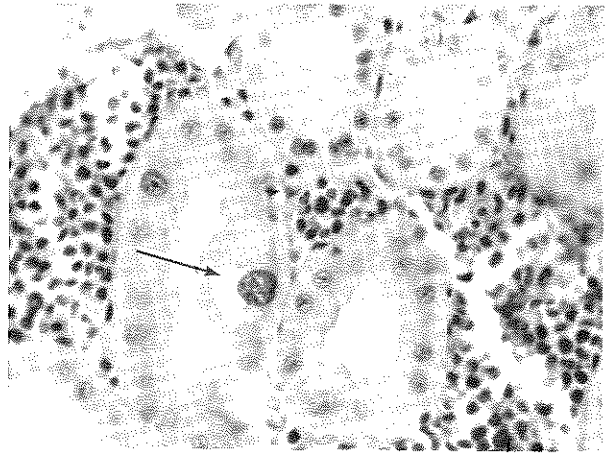

Figure G12. Megalokaryosis and megalocytosis in proximal tubule of kidney (arrow): 8W:0.1 x400.

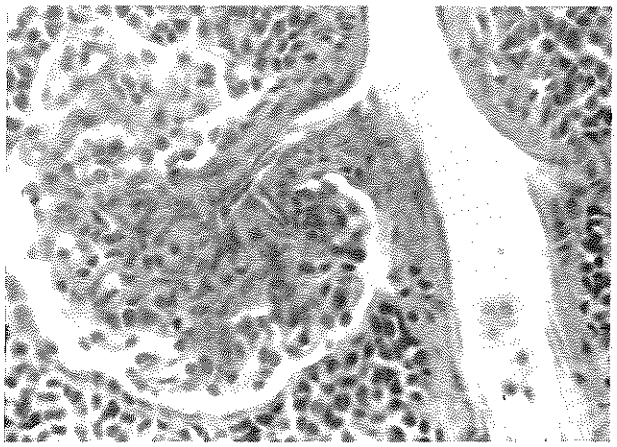

Figure G13. Normal renal corpuscle: initial control x400.

Figure G14. Mesangiolysis: initial control x200.

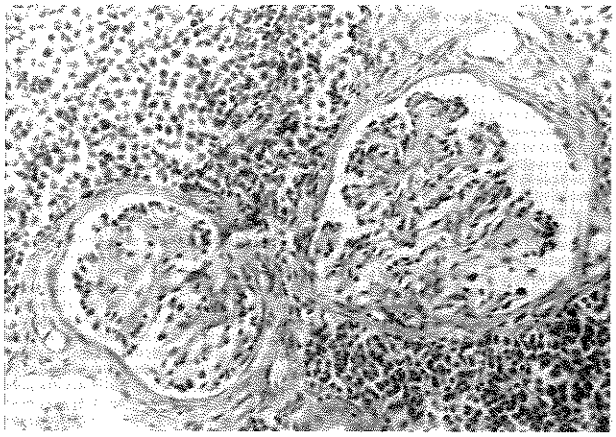

Figure G15. Mesangiosclerosis of two renal corpuscles: 16W:1.0 x200.

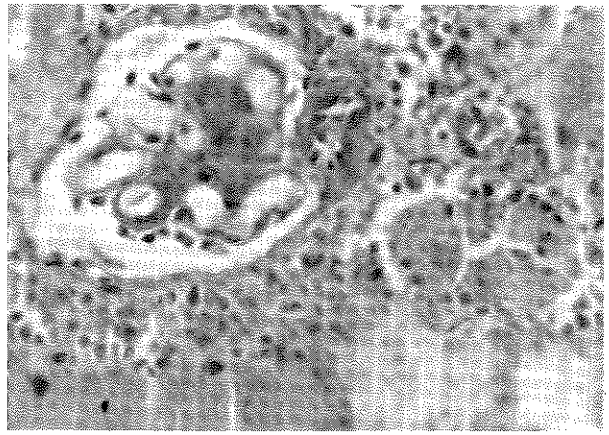

Figure G16. Membranous glomerulonephritis: 4W:1.0 x400.

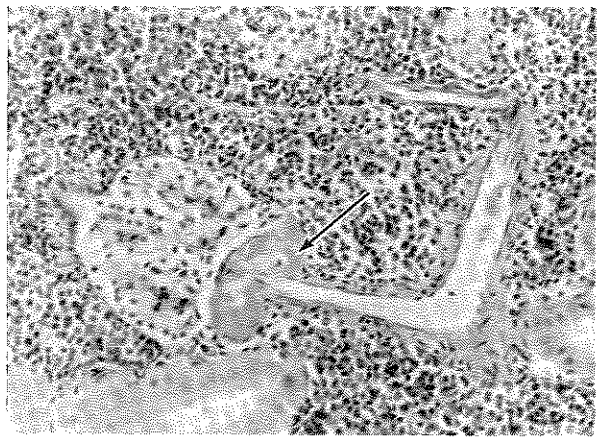

Figure G17. Periarteriolar fibrinoid degeneration (arrow): 16W:0.1 x200.

Membranous Glomerulonephritis. The most characteristic feature of this condition is a marked thickening of the visceral epithelum's basal lamina. Hence, glomerular capillaries appear to have dilated lumina that are surrounded by a concentric layer of homogenous, eosinophilic substance (Figure G16). Little, if any, cellular proliferation accompanies this particular lesion.

Periarteriolar Fibrinoid Degeneration. Often accompanied by mesangiolysis and/or mesangiosclerosis, this peculiar idiopathy involves focal degeneration at the vascular pole of the renal corpuscle. Where afferent and efferent arterioles would normally approximate one another, all cellular detail is lost and only an amorphous, eosinophilic material remains (Figure G17).

Liver

Normal scorpionfish liver is not admixed with pancreatic tissue, as it is in other species of fish (Perkins et al. 1982). Hepatic parenchyma assumes the configuration of lobules, each of which consists of cords (muralia) of hepatocytes that are radially disposed about a central vein (Figure G18). Situated between all apposing cords of hepatocytes are endothelial-lined venous sinusoids that convey blood inward, towards the central vein. This architectural arrangement of parenchyma and blood vessels may be likened to spokes converging on the hub of a wheel.

Scattered throughout the hepatic parenchyma are bile ductules (cholangioles) and larger, intrahepatic bile ducts (Figure G19). Although venous sinusoids are devoid of endemic populations of phagocytic reticuloendothelial Kupffer cells, connective tissue phagocytes abound--as is evidenced by circumscribed aggregates of cellular debris resulting from their activities. Called melanin macrophage centers, their numbers and size vary in tissues of both the liver and kidney (Figure G19).

Hepatic lesions recorded during the course of this experiment rival the spectrum of idiopathies earlier reported in the kidney. Chief among these were hepatocyte hypertrophy (focal hypertrophy) and extensive fatty vacuolation. Less common were incidences of hepatocellular nuclear pyknosis or pleomorphism, megalocytic hepatosis, focal hepatocellular hyperplasia, sclerosis or necrosis, cholangioproliferative foci, and parasitic myxosporidian involvement of cholangioles and intrahepatic bile ducts. For the sake of brevity, the following description will be restricted to the most prominent hepatocellular alterations: hypertrophy and vacuolation.

Hepatocyte Hypertrophy and Vacolation. Focal hepatocellular hypertrophy involves an increase in cell size, without a concomitant

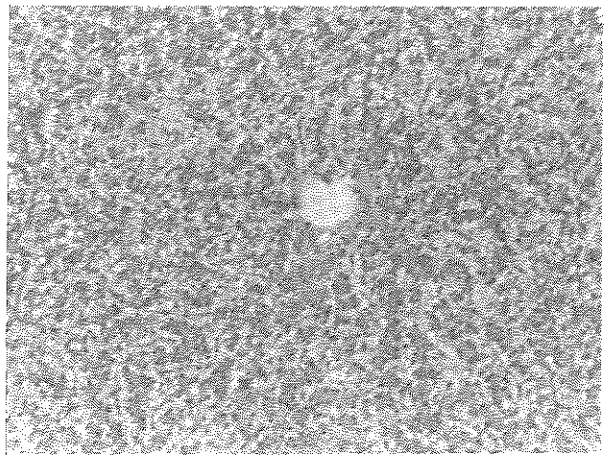

Figure G18. Normal hepatic parenchyma, arranged around a central vein: 4W:1.0 x100.

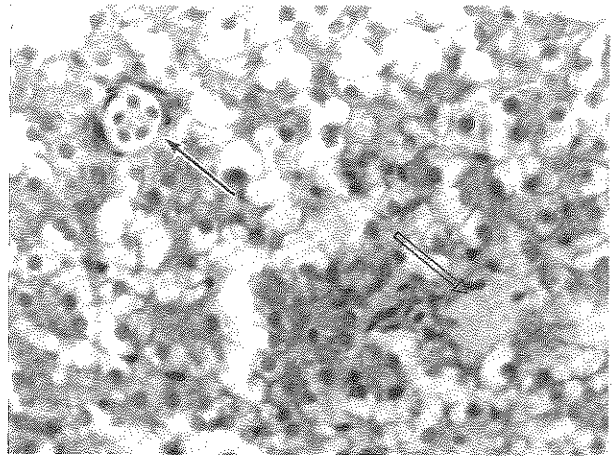

Figure G19. Normal hepatic parenchyma, cholangiole (black arrow), and melanin macrophage center (clear arrow): 4W:C x400.

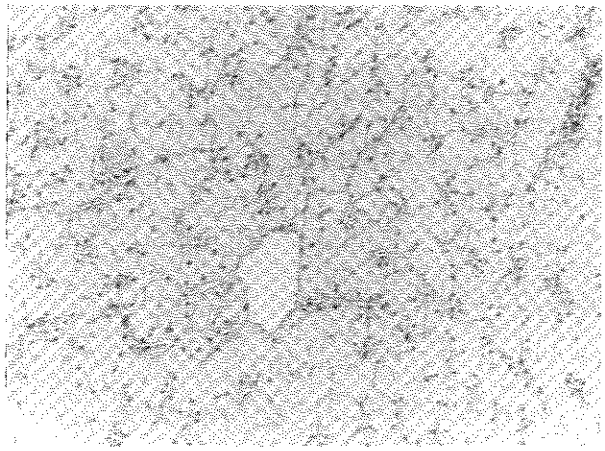

Figure G20. Marked hypertrophy and vacuolation of hepatic parenchyma: 4W:1.0 x100.

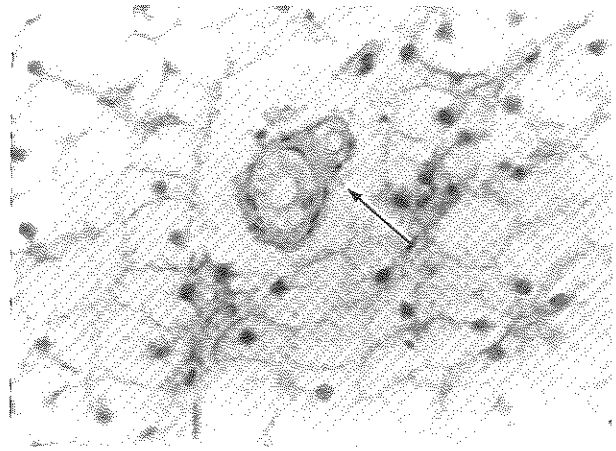

Figure G21. Marked hypertrophy and vacuolation of hepatic parenchyma, as well as cholangioles (arrow): 4W:1.0 x400.

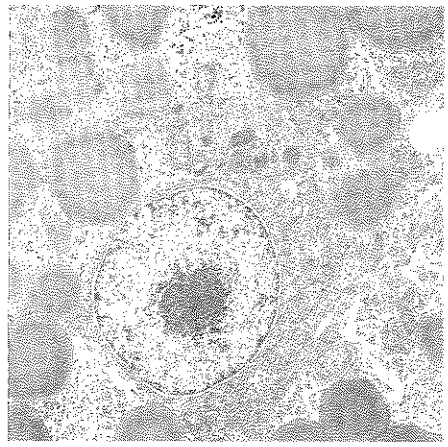

Figure G22. Transmission electron micrograph of moderately vacuolated hepatocytes, illustrating osmiophilic lipid droplets: 8W:C x6,200.

increase in nuclear size (Figures G18-G21). This condition was invariably accompanied by extensive hepatocellular fatty accumulation--so widespread and pronounced that, at times, even cholangioles were vacuolated (Figure G21). That lipid was responsible for such vacuolation was confirmed by electron microscopy (Figure G22). Sinusoidal congestion often occurred in the company of both of these conditions (Figure G20).

LITERATURE CITED

Bay, S.M., D.J. Greenstein, G.P. Hershelman, C.F. Ward, and D.A. Brown. 1984a. The effectiveness of cadmium detoxification by scorpionfish. IN: This Volume.

Bay, S.M., D.J. Greenstein, and P. Szalay. 1984b. Biological effects of cadmium detoxification. IN: This Volume.

Brown, D.A., K.D. Jenkins, E.M. Perkins, R.W. Gossett, and G.P. Hershelman. 1982. Detoxification of metals and organic compounds in white croakers. pp. 157-172 IN: SCCWRP Biennial Report, 1981-1982, W. Bascom (ed.). Long Beach, Calif.

Gardner, G.R., and P.P. Yevich. 1970. Histological and hematological responses of an estuarine teleost to cadmium. J. Fish. Res. Board Canada 27: 2185-2196.

Haensly, W.E., J.M. Neff, J.R. Sharp, A.C. Morris, M.F. Bedgood, and P.D. Boem. 1982. Histopathology of *Pleuronectes platessa* L. from Aber Wrac'h and Aber Benoit, Brittany, France: long-term effects of the "Amoco Cadiz" crude oil spill. J. Fish Diseases 5:365-391.

Hickman, C.P., and B.F. Trump. 1969. The kidney: pp. 125-126 IN: Fish Physiology, Vol 1, W.S. Hoar and D.J. Randall (eds.). Academic Press, New York.

Humason, G.L. 1972. Animal Tissue Techniques, 3rd ed. W.H. Freeman and Co., San Francisco, Calif. 641 pp.

Luna, L.G. (ed.). 1968. Manual of Histologic Staining Methods of the Armed Forces Institute of Pathology, 3rd ed. The Blakiston Division, McGraw-Hill, New York. 258 pp.

Lyman, O.H. 1977. An Introduction to Statistical Methods and Data Analysis. Wadsworth Publ. Co., Belmont, Calif. pp. 320-321.

McCain, B.B., M.S. Meyers, U. Varanasi, D.W. Brown, L.D. Rhodes, W.D. Gronlund, D.G. Elliott, W.A. Palsson, H.O. Hodgins, and D.C. Malins. 1982. Pathology of two species of flatfish from urban estuaries in Puget Sound, DOC/EPA Interagency Energy/Environment R & D Program Report, Boulder, Colo. 100 pp.

Malins, D.C., B.B. McCain, D.W. Brown, A.K. Sparks, and H.O. Hodgins (eds.). 1980. Chemical contaminants and biological abnormalities in central and southern Puget Sound. Technical Memorandum OMPA-2, National Oceanic and Atmospheric Administration, Boulder, Colo. 295 pp.

Perkins, E.M., D.A. Brown, and K.D. Jenkins. 1982. Contaminants in white croakers *Genyonemus lineatus* (Ayres, 1855) from the southern California Bight: III. Histopathology. pp. 215-231 IN: Physiological Mechanisms of Marine Pollutant Toxicity, W.B. Vernberg, A. Calabrese, F.P. Thurberg, and F.J. Vernberg (eds.). Academic Press, New York.

Perkins, E.M., D. Ebenstein, D.A. Brown, K.D. Rosenthal, and A. Sassoon. In Preparation. The discovery of renal corpuscles in the hemopoietic kidney of the California scorpionfish *(Scorpaena guttata Girard)*. Copeia.

Ribelin, W.E., and G. Migaki (eds.). 1975. The Pathology of Fishes. The University of Wisconsin Press, Madison. 1004 pp.

Roberts, R.J. (ed.). 1978. Fish Pathology. Bailliere Tindall/Cassell Ltd., London. 318 pp.

SAS Institute, Inc. 1982. SAS User's Guide: Statistics. Cary, N.C.

Slooff, W., C.F. vanKreijl, and A.J. Baars. 1983. Relative liver weights and xenobiotic-metabolizing enzymes of fish from polluted surface waters in the Netherlands. Aquatic Toxicol. 4:1-14.

Yasutake, W.T., and J.H. Wales. 1983. Microscopic Anatomy of Salmonids: An Atlas. Resource Publication 150, Fish and Wildlife Service, Washington, D.C. pp. 97-103.